Journal of Bone and Mineral Metabolism
https://doi.org/10.1007/s00774-020-01102-4

ORIGINAL ARTICLE

Marine collagen scaffolds and photobiomodulation on bone healing process in a model of calvaria defects

M. A. Cruz[1] · K. R. Fernandes[1] · J. R. Parisi[2] · G. C. A. Vale[1] · S. R. A. Junior[1] · F. R. Freitas[1] · A. F. S. Sales[1] · C. A. Fortulan[2] · O. Peitl[2] · E. Zanotto[2] · R. N. Granito[1] · A. M. Ribeiro[1] · A. C. M. Renno[1]

Received: 2 December 2019 / Accepted: 23 March 2020

Abstract

Introduction Collagen from marine esponges has been used as a promising material for tissue engineering proposals. Similarly, photobiomodulation (PBM) is able of modulating inflammatory processes after an injury, accelerating soft and hard tissue healing and stimulating neoangiogenesis. However, the effects of the associated treatments on bone tissue healing have not been studied yet. In this context, the present study aimed to evaluate the biological temporal modifications (using two experimental periods) of marine sponge collagen or sponging (SPG) based scaffold and PBM on newly formed bone using a calvaria bone defect model.

Material and Methods Wistar rats were distributed into two groups: SPG or SPG/PBM and euthanized into two different experimental periods (15 and 45 days post-surgery). A cranial critical bone defect was used to evaluate the effects of the treatments. Histology, histomorfometry and immunohistological analysis were performed.

Results Histological findings demonstrated that SPG/PBM-treated animals, 45 days post-surgery, demonstrated a higher amount of connective and newly formed bone tissue at the region of the defect compared to CG. Notwithstanding, no difference among groups were observed in the histomorphometry. Interestingly, for both anti-transforming growth factor-beta (TGF-β) and anti-vascular endothelial growth factor (VEGF) immunostaining, higher values for SPG/PBM, at 45 days post-surgery could be observed.

Conclusion It can be concluded that the associated treatment can be considered as a promising therapeutical intervention.

Keywords Bone healing · Marine sponges · Collagen · Biomaterials · Histomorphometry · Photobiomodulation

Introduction

The use of collagen-based biomaterials in the field of tissue engineering applications has been intensively growing over the past decades [1, 2]. Based on its biocompatibility, low immunogenicity and mechanical properties, collagen-derived grafts are extremely suitable can be used as bone grafts for stimulating healing, as carriers for drug delivery, as bone substitutes, antithrombogenic surfaces and immobilization of therapeutic enzymes [3–5].

Collagen can be extracted from various sources but the most common are the ones from bovine and porcine skin and bones [3, 4]. However, they have been considered a great pathological risk for transmitted diseases, very challenging in the extraction process and presenting high costs [6]. More recently, marine life has formed a considerable source of collagen, which can be extracted from fishes, crabs and sponges [3]. In this context, marine sponge collagen or sponging (SPG), which is analogous to the human collagen type XIII, is one of the most promising to be used for biomedical applications, being safe and easy to extract [7]. Many studies have demonstrated that marine collagen is a suitable framework for cell attachment and proliferation of osteoblasts [8–10].

Similarly, another very promising resource that has been used for stimulating tissue metabolism is the photobiomodulation (PBM) [11–13]. PBM is able of modulating inflammatory processes after an injury, accelerating soft and hard

✉ M. A. Cruz
allmayda07@gmail.com

[1] Department of Biosciences, Federal University of São Paulo (UNIFESP), Santos, Brazil

[2] Department of Fisiotherapy, Federal University of São Carlos (UFSCar), São Carlos, Brazil

Published online: 18 April 2020

tissue healing and stimulating neoangiogenesis [14–16]. The action of PBM can be explained mainly by the interaction of light and tissues, which generates a series of modifications in cell metabolism, including stimulation of mitochondrial respiration and increasing in the synthesis of ATP [13, 17–19]. These effects can culminate in the increased expression of genes related to protein synthesis, cell migration and proliferation, anti-inflammatory signaling, anti-apoptotic proteins and antioxidant enzymes [13, 20–22].

Based on these effects, this therapeutical intervention has been also used to stimulate bone metabolism and fracture consolidation [11, 23, 24]. An increased expression of genes related to bone differentiation (BMP4, ALP and RUNX-2) was observed after PBM in an experimental model of bone defects in rats [25]. Moreover, microarray analysis demonstrated that PBM produced an upregulation of genes related to the inflammatory process (MMD, PTGIR, PTGS2, Ptger2, IL1, 1IL6, IL8, IL18) and angiogenic activities (FGF14, FGF2, ANGPT2, ANGPT4 and PDGFD) in an experimental model of tibial bone defects in rats [26].

However, no study was found investigating the effects of the association of both therapies in the process of bone healing. In view of the aforementioned, it was hypothesized that the treatment using both therapies would be able of accelerating tissue metabolism, stimulating bone healing. Consequently, the present study aimed to evaluate the biological temporal modifications (using two experimental periods) of SPG based scaffold and PBM on newly formed bone using a calvaria bone defect model trough histological, histomorfometry and immunohistological analysis were performed.

Material and methods

Aplysina fulva was used for marine collagen extraction collected in Praia Grande (23° 49′ 23.76″ S, 45° 25′ 01.79″ W, São Sebastião, Brazil). The method was described by Swatschek et al. [27]. Briefly, after collection, sponges were washed with Milli-Q water (three times) and cut in small pieces of sponges. Afterwards, samples were inserted in a stirred beaker with Tris–HCl buffer and pH was adjusted to nine with (with the addition of NaOH). Solution was kept in agitation for 24 h and centrifuged for 5 min (at 2 °C). Then, the pellet was discarded and the supernatant removed. Afterwards, pH was adjusted again to four (using acetic acid solution) and the precipitate obtained was resuspended in Milli-Q water, centrifuged and lyophilized for preservation.

Additionally, for scaffold manufacturing carboxymethyl cellulose (CMC) (density 1.59 g/cm^3, Sigma Aldrich, Missouri, USA), Poly (methyl methacrylate) (PMMA, particle size: 15 µm, VIPI Produtos Odontológicos (Pirassununga, São Paulo, Brazil) and methyl methacrylate (MMA, purity: 99.09%, VIPI Produtos Odontológicos, Pirassununga, São Paulo, Brazil) were used. (the polymers were used with the purpose of aggregating BS and SPG).

Scaffold preparation

Scaffolds of marine collagen were manufactured following the methodology of Parisi et al. [7]. For this, PMMA was used for aggregating the materials and CMC was used to produce pores into samples (around 60%) [28–30]. SPG were weighted (Table 1) and mixed in a container with distilled water, using a spatula. Subsequently, MMA monomer was added, mixture again and the paste was transferred to a silicon mold (8 mm × 2 mm). Molds were then sealed, submitted to a pressure air chamber (at 0.6 MPa) for 30 min and vacuum dried (10^{-3} Torr) for 15 min. Samples were then, removed from the silicon molds, packaged and sterilized by ethylene oxide (Acecil, Campinas, SP, Brazil). The proportion of materials used in manufacturing process was PMMA (0.236 g), MMA (0.472 g), SPG (0.268 g), CMC (0.043 g) and water (0.565 g).

In vivo studies

In the present study, male Wistar rats (12 weeks, weight 300–350 g) were distributed into two groups ($n = 12$): spongin group (SPG) and spongin PBM group (SPG/PBM). Two sub-groups were created, with different times of euthanasia (15 and 45 days). Animals were maintained under light–dark periods of 12 h, controlled temperature (22 ± 2 °C), with free access to water and standard food.

Surgical procedures

All animals were submitted to anaesthesia with a combination of ketamine (80 mg/kg), xylazine (8 mg/kg), acepromazine (1 mg/kg) and fentanyl (0.05 mg/kg). For the surgical procedure, animals had their skulls washed, shaved and disinfected with povidone-iodine. After the incision, the periosteum was removed and the parietal region was exposed.

Table 1 PBM parameters

Parameters	Values
Power	30 mw
Wavelength	808 nm (infrared)
Mode of action	Continuous
Beam transverse area	0.028 cm^2
Energy density	30 J/cm^2
Time	28 s
Energy	0.8 J
Application mode	Stationary in skin contact mode

Afterwards, an 8 mm defect was created using a trephine drill (3i Implant Innovations Inc., Palm Beach Gardens, USA) under copious saline irrigation and the implants were inserted in the created defect, according to a randomization scheme. Wounds were closed with resorbable Vicryl® 5-0 (Johnson & Johnson, St.Stevens-Woluwe, Belgium). Four animals were housed per cage and all the water and food intaken were monitored in the initial post-operative period. Rats were given appropriate postoperative care and animals were observed for signs of pain, infection and proper activity. After the experimental periods, animals were euthanized by $CO_{2,}$ for sample removal.

PBM treatment

A Photon Lase III equipment (DMC, São Carlos, Brazil) was used for this study as described in Table 1. After the surgical procedure, irradiation was initiated at on single point in the center of the region of the bone defect, through the contact pontial technic. Three applications per week were performed, in non-consecutive days, (in a total of 6 and 18 sessions) for 15 and 45 days, respectively. It is important to emphasize that the PBM parameters were chosen based on the previous work of our group [31].

Histological procedures

After the removal, samples were submitted to a standard protocol based on fixing in formaldehyde (24 h), followed by dehydration in ethanol and embedding in methylmethacrylate (MMA). After these procedures, histological laminaes were obtained (thin sections 5 µm), in a perpendicular direction, to the medial–lateral drilling axis of the implants) using a microtome with a tungsten carbide disposable blade (Leica TC65, Leica Microsystems SP 1600, Nussloch, Germany). Goldner Trichrome was used for staining the samples and at least three sections of each specimen were examined using light microscopy (Leica Microsystems AG, Wetzlar, Germany).

Qualitative and histomorphometric analysis

The qualitative analysis was performed considering the following parameters: presence of granulation tissue, newly formed bone, the presence of osteoid and particles of biomaterial. Analysis was performed in a blinded way by two experienced observed (M.A.C. and S.R.J.)

The semi-automatic image-analysing OsteoMeasure System (Osteometrics, Atlanta, USA) was used for quantitatively score all the samples. The mean tissue area analysed was 2.879 ± 0.674 mm^2, covering the entire region of the surgically created bone defect. After analysis, the following parameters were obtained: bone volume as a percentage of tissue volume (BV/TV %), osteoid volume as a percentage of tissue volume (OV/TV %) and the number of osteoblasts per unit of tissue area (N.Ob/T.Ar/mm^2) In addition, the analysis was performed by one experienced observer (G.C.A.V.), in a blinded way.

Immunohistochemistry analysis

For immunohistochemistry analysis, resin from the samples was removed with xylene/chloroform, rehydrated in ethanol and pretreated with 0.01 M citric acid buffer (pH 6) in a steamer for 5 min. Peroxidase was inactivated using hydrogen peroxide in phosphate-buffered saline (PBS) for 5 min. Primary antibody was incubated with anti-vascular endothelial growth factor (anti-VEGF, Santa Cruz Biotechnology, USA, the concentration of 1:200) and anti-transforming growth factor beta (anti-TGF-β, Santa Cruz Biotechnology, USA, at a concentration of 1:200), for 2 h. Antibody anti-rabbit IgG (Vector Laboratories, Burlingame, CA, USA) was used for 30 min and samples were incubated (30 min). A solution of 3-3′-diaminobenzidine solution was used to reveal the immunostaining (5 min) and restained with Harris haematoxylin. Qualitative analysis was used to investigate the presence and location of the immunomarkers and is performed using a light microscopy (Leica Microsystems AG, Wetzlar, Germany). Furthermore, semi-quantitative evaluation was performed following the score: 1 = absent (0% of immunostaining), 2 = weak (1–25% of immunostaining), 3 = moderate (36–67% of immunostaining) and 4 = intense (68–100% of immunostaining) [12]. Analysis was performed in a blinded way (G.C.A.V. and J.R.P.).

Statistical analysis

Data were analysed and displayed in graphs, and the values expressed as mean and standard deviation. In the statistical analysis, the distribution of variables was tested using the Shapiro–Wilk normality test. For the analysis of multiple comparisons, ANOVA was used with post hoc Tukey for parametric data and nonparametric data, the Kruskal–Wallis test was used with post hoc Dunn. The level of significance was set at 5% ($p \leq 0.05$). All statistical analyses were performed using GraphPad Prism version 6.01.

Results

Histopathological analysis

For SPG, at 15 days after the surgical procedures, bone effect was filled mainly by particles of the material (which presented some degradation). Moreover, connective tissue and inflammatory infiltrate also could be seen with some

areas of newly formed bone. In the second experimental period, neoformed bone tissue was observed filling most of the defect, with some scarce areas of connective tissue and material particles (magnification of 20 ×) (Fig. 1).

For SPG/PBM, at 15 days post-surgery, bone defect was filled by material particles, undergoing on a degradation process. Furthermore, the connective tissue around the material, granulation tissue interspersing the material particles and some inflammatory infiltrate areas. New formed tissue areas were seen close to the cortical bone. In the second experimental period, extensive connective tissue formation, with the presence of few material particles and areas of newly formed bone were seen almost all over de bone defect (magnification of 20 ×) (Fig. 1).

Histomorphometry

Figure 2 demonstrates the data of the histomorphometry analysis. No difference was obtained in the parameters BV/TV (%) and OV/TV (%) between the experimental groups and periods. Moreover, higher values were found for N.ob/T.Ar (mm^2) for SPG/PBM 15 days post-surgery compared to SPG 45 days post-surgery.

Immunohistochemistry analysis

TGF-β immunostaining

The qualitative analysis of TGF-β expression for all the experimental groups, after 15 and 45 days of surgery is demonstrated in Fig. 3.

In the first period analyzed, for both experimental groups, a similar pattern of TGF-β immunoexpression could be observed, mainly in the granulation tissue and around the particles of the materials in the bone defect (Fig. 3a, b). Additionally, 45 days post-surgery, it is possible to observe that TGF-β immunolabeling continues in the granulation tissue, mainly at the center of the defect and around the particles of the materials (Fig. 3c, d).

Semi-quantitative analysis of TGF-β immunostaining after 15 and 45 days post-surgery was shown in Fig. 4. No difference among the experimental groups was observed in the first period analyzed. Furthermore, after 45 days post-surgery, it is possible to observe higher immunolabelling of TGF-β for SPG/PBM compared to SPG ($p < 0.05$).

VEGF immunostaining

Figure 5 demonstrated the VEGF immunolabeling, after 15 and 45 days post-surgery. VEGF immunolabeling was seen predominantly in the granulation tissue and around the particles of the materials for both groups 15 days post-surgery

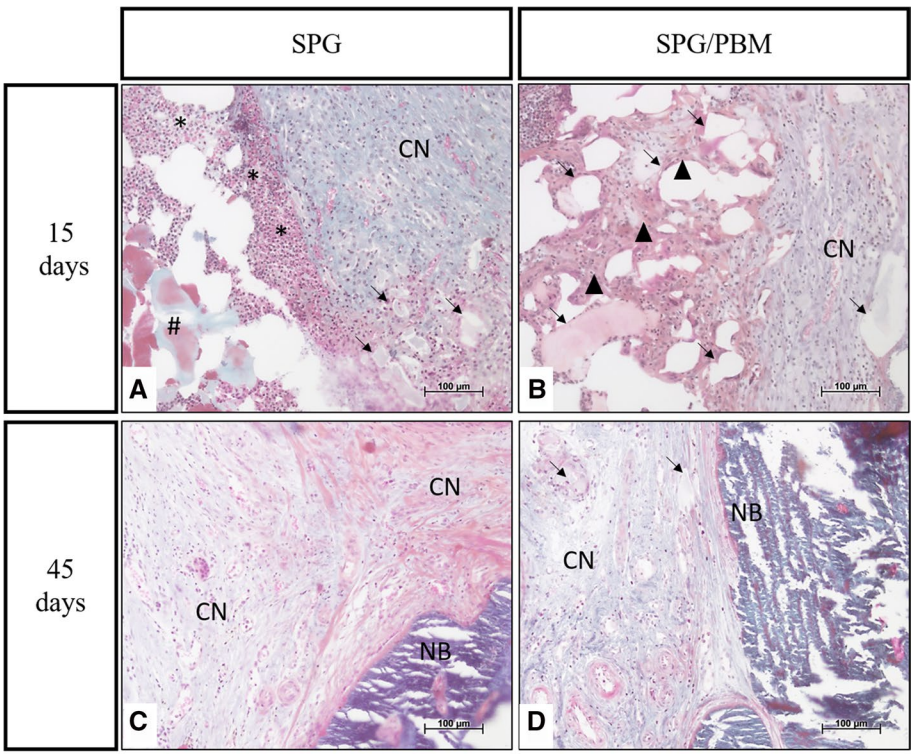

Fig. 1 Representative histological sections of SPG ($n = 6$) and SPG/PBM ($n = 6$) experimental groups, after 15 and 45 days post-surgery Goldner's trichome staining. New formed bone tissue (NB), connective tissue (CN), inflammatory infiltrate (*), biomaterial (#), granulation tissue (▲) and material particles undergoing degradation process (arrow)

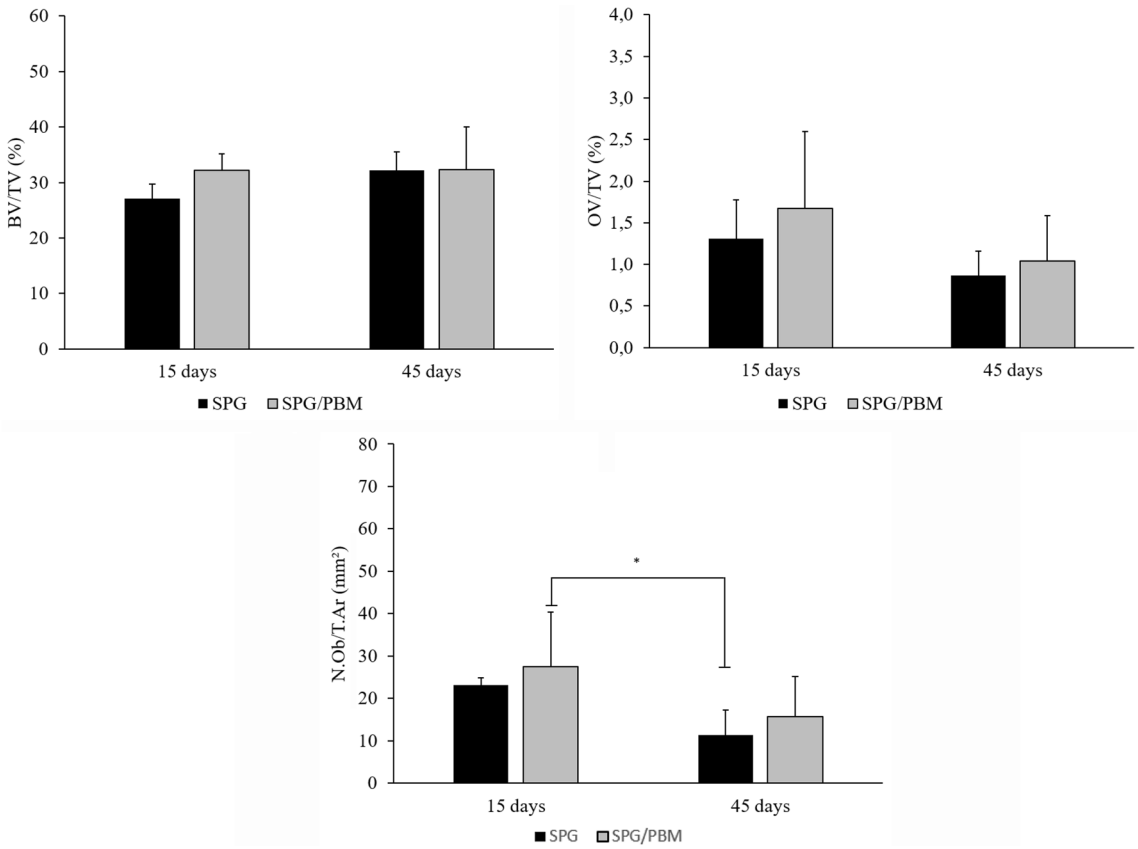

Fig. 2 Means and standard errors of histomorphometry. BV/TV, OV/TV and N.Ob/T.Ar. ANOVA was used with post hoc Tukey, $*p < 0.05$

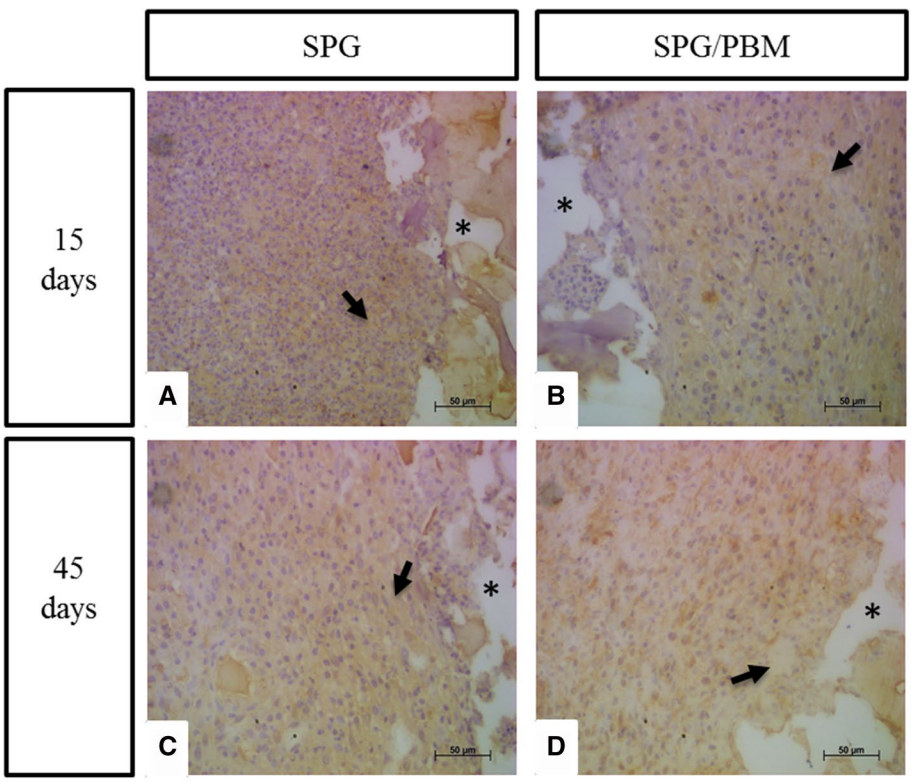

Fig. 3 Representative histological sections of Transform Growth Factor Beta (TGF-β) immunohistochemistry of the SPG and SPG/PBM experimental groups, after 15 and 45 days post-surgery. TGF- β immunostaining (arrow) and biomaterial (*). Scale bar: 50 µm (mag. × 40)

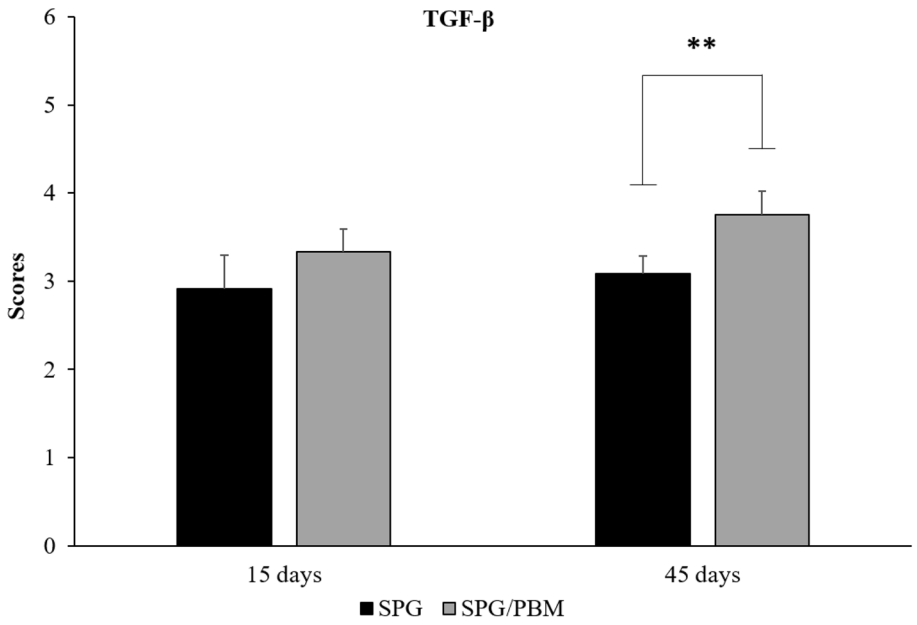

Fig. 4 Means and standard errors of the immunohistochemistry analysis of TGF-β. test *t*. $p < 0.05$

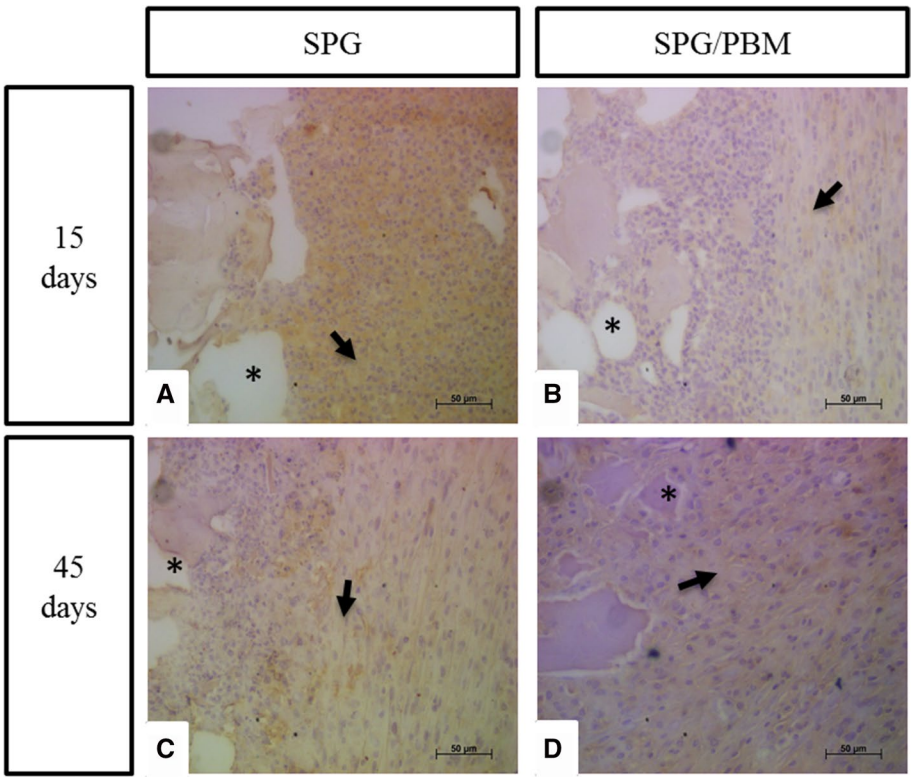

Fig. 5 Representative histological sections of VEGF immunohistochemistry for SPG and SPG/PBM experimental groups, 15 and 45 days post-surgery. Biomaterial (*) and VEGF immunostaining (arrow). Scale bar: 50 µm (mag. × 40)

(Fig. 4a, b). After 45 days of surgery, VEGF immunostaining still could be observed in the granulation tissue and around the particles of the materials, especially in the center of the defect (Fig. 5c, d).

Figure 5 shows the results of the semi-quantitative analysis of VEGF in both periods analyzed. At 15 days post-surgery, no significant difference among the experimental groups was observed. Additionally, 45 days post-surgery, it was possible to observe a significantly higher immunolabelling of VEGF expression for SPG/PBM compared to SPG ($p = 0.05$).

Discussion

In this study, the biological effects of SPG associated with PBM on bone healing in a critical experimental model in the calvaria of rats were evaluated. It was hypothesized that the combined therapy would be able to upregulate the immunostaining markers related to cell differentiation and angiogenesis, which could culminate in increasing bone deposition. Histological findings demonstrated that SPG/PBM treated animals, 45 days post-surgery, demonstrated a higher amount of connective and newly formed bone tissue at the region of the defect compared to CG. However, the histomorphometry showed no difference among groups. Interestingly, for both TGFβ and VEGF immunostaining, higher values for SPG/PBM, at 45 days post-surgery could be observed (Fig. 6).

It is well known that collagen, including SPG, represents a unique material to be used in the area of bone tissue engineering field, presenting stimulatory effects on tissue metabolism [3, 27]. Similarly, PBM constitutes a very promising therapeutical intervention, capable of stimulating bone tissue and producing healing [12, 32, 33].

Although the lack of difference in the histomorphometry analysis, the qualitative histology pointed out that the animals treated with the combined treatment presented a more organized tissue pattern, with the bone defects being filled with newly formed bone and connective tissue. As mentioned before, both therapies have stimulatory effects on bone metabolism. Consequently, the more organized tissue pattern in this group may be explained by the fact that the association of SPG and PBM was able of stimulating mesenchymal cells and osteoblasts, culminating in the increase of newly formed bone deposition, producing tissue healing of the cranial bone defect. Moreover, Freitas et al. [34] and Oliveira et al. [35] demonstrated the beneficial effect of PBM and collagen membranes for stimulating bone healing using animal experiments. Although the positive biological effects of the associated treatment, the lack of difference in the histomorphometry analysis may be explained by the post-surgery period analyzed, using a critical bone defect. Possibly, a higher difference would be seen if a longer period were used, especially considering the size of the defect which demands a higher period for healing.

The immunohistochemistry analysis demonstrated an increased immunolabeling of TGFb in SPG/PBM, 45 days post-surgery. TGFb stimulates matrix protein synthesis and bone cell proliferation, having a critical role in bone remodeling [36]. In this context, the higher immunolabelling observed for animals which received the associated treatments may have had a positive effect on the activity and proliferation of osteoblast cells, which may have influenced newly formed bone deposition at this period. Oliveira et al. (2017) demonstrated a more intense immunostaining for TGF-β in critical bone defects in rats after treatment with collagen associated to PBM (at 120 J/cm^2), stating that the associated treatments could offer a synergistic advantage in improving the healing of bone fractures.

Furthermore, an appropriate vascularization is essential to allow an adequate bone healing process [37]. It is well known that VEGF is the main mediator during the process of angiogenesis and the formation of newly blood vessels [16, 38]. In the present study, a higher immunolabelling

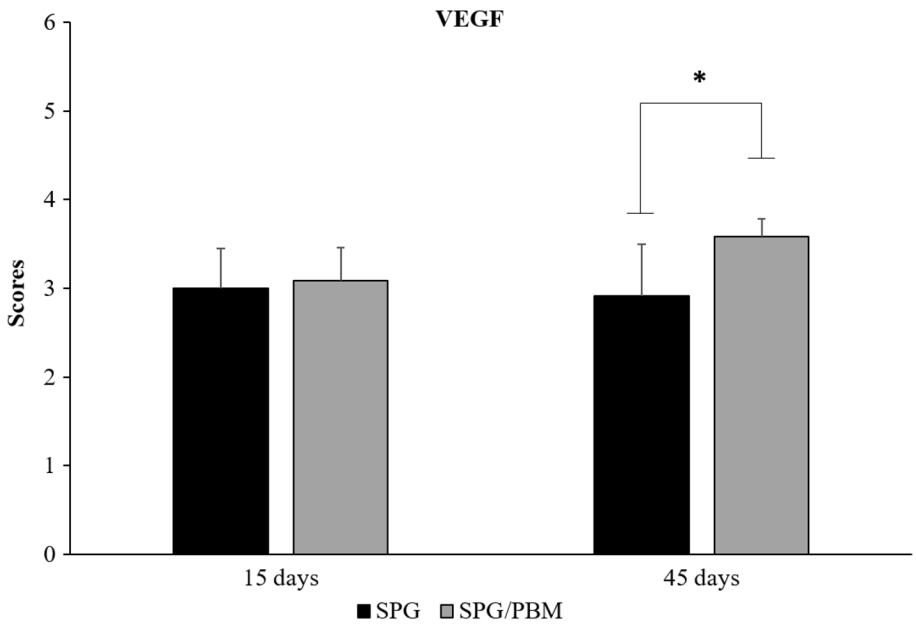

Fig. 6 Means and standard errors of the immunohistochemistry analysis of VEGF. Test *t*. *$p < 0.05$

presented by SPG/PBM animals, at the second experimental period, may be related to the higher number of blood vessels, increasing irrigation and accelerating healing. It has been reported that PBM has a stimulatory effect on neovascularization by stimulating the secretion of angiogenic factors, [39] which together with the biological properties of SPG might further influence bone formation.

Although the positive evidences, the present work was limited to a relatively short period post-surgery. Based on the higher immunolabbeling of TGFb and VEGF at 45 days post-surgery, possibly more positive results could be seen if longer periods after the surgical procedure were used. In this context, the long-term biological performance of SPG/PBM needs to be clarified. Following this strategy, which involves the combination of a biomaterial and a subsequent treatment, further investigations are necessary to validate these combinations as safe and efficient materials for biomedical applications.

From the data of the present study, it can be concluded that the associated treatment can be considered as a promising therapeutical intervention based on the positive effects on the immunolabeling of TGFb and VEGF and induced a higher deposition of newly formed bone and material degradation. However, longer periods of post-surgery should be evaluated.

Acknowledgements Authors would like to thank Fundação de Amparo à Pesquisa do Estado de São Paulo (FAPESP) for the scholarship (grant no. 2016/13636-9). This research was supported by fellowships from Coordenação de Aperfeiçoamento de Pessoal de Nível Superior (CAPES)—Finance Code 001.

Compliance with ethical standards

Conflict of interest The authors declare that they have no conflict of interest.

Ethical approval The Animal Care Committee guidelines of the Federal University of São Paulo (CEUA no. 4331220318) approved the present study and national guidelines for the care and use of laboratory animals were observed.

Informed consent No informed consent.

References

1. Blais M, Parenteau-Bareil R, Cadau S, Berthod F (2013) Concise review: tissue-engineered skin and nerve regeneration in burn treatment. Stem Cells Transl Med 2:545–551
2. Pozzolini M, Scarfì S, Gallus L, Castellano M, Vicini S, Cortese K et al (1847) Production, characterization and biocompatibility evaluation of collagen membranes derived from marine sponge chondrosia reniformis Nardo. Mar Drugs 2018:111–131
3. Silva TH, Moreira-Silva J, Marques ALP, Domingues A, Bayon Y, Reis RL (2014) Marine origin collagens and its potential applications. Marine Drugs 16:5881–5901
4. Lin Z, Solomon KL, Zhang X, Pavlos NJ, Abel T, Willers C et al (2011) In vitro evaluation of natural marine sponge collagen as a scaffold for bone tissue engineering. Int J Biol Sci 7:968–977
5. Zdarta J, Norman M, Smułek W, Moszyński D, Kaczorek E, Stelling AL et al (2017) Spongin-based scaffolds from Hippospongia communis demosponge as an effective support for lipase immobilization. Catalysts 7:147–167
6. Widdowson JP, Picton AJ, Vince V, Wright CJ, Mearns-Spragg A (2018) In vivo comparison of jellyfish and bovine collagen sponges as prototype medical devices. J Biomed Mater Res Part B Appl Biomater 106:1524–1533
7. Parisi JR, Avanzi IR, Santana AF, Renno ACM, Andrade AL, Fortulan CA et al (2018) Incorporation of collagen from marine sponges (spongin) into hydroxyapatite samples: characterization and in vitro biological evaluation. Mar Biotechnol 21:30–37
8. Exposito JY, Cluzel C, Garrone R, Lethias C (2002) Evolution of collagens. Anat Rec 268:302–316
9. Green D, Howard D, Yang X, Kelly M, Oreffo ROCOC (2003) Natural marine sponge fiber skeleton: a biomimetic scaffold. Tissue Eng 9:1156–1166
10. Iwatsubo T, Kishi R, Miura T, Ohzono T, Yamaguchi T (2015) Formation of hydroxyapatite skeletal materials from hydrogel matrices via artificial biomineralization. J Phys Chem B 119:8793–8799
11. Tim CR, Pinto KNZ, Rossi BRO, Fernandes K, Matsumoto MA, Parizotto NA et al (2014) Low-level laser therapy enhances the expression of osteogenic factors during bone repair in rats. Lasers Med Sci 29:147–156
12. Magri AMP, Fernandes KR, Assis L, Mendes NA, da Silva Santos ALY, de Oliveira DE et al (2015) Photobiomodulation and bone healing in diabetic rats: evaluation of bone response using a tibial defect experimental model. Lasers Med Sci 30:1949–1957
13. Hamblin MR (2018) Mechanisms and mitochondrial redox signaling in photobiomodulation. Photochem Photobiol 94:199–212
14. Diniz IMA, Carreira ACO, Sipert CR, Uehara CM, Moreira MSN, Freire L et al (2018) Photobiomodulation of mesenchymal stem cells encapsulated in an injectable rhBMP4-loaded hydrogel directs hard tissue bioengineering. J Cell Physiol 233:4907–4918
15. Hak DJ, Fitzpatrick D, Bishop JA, Marsh JL, Tilp S, Schnettler R et al (2014) Delayed union and nonunions: Epidemiology, clinical issues, and financial aspects. Injury [Internet] 45:S3–7. https://doi.org/10.1016/j.injury.2014.04.002
16. Ruh AC, Frigo L, Cavalcanti MFXB, Svidnicki P, Vicari VN, Lopes-Martins RAB et al (2018) Laser photobiomodulation in pressure ulcer healing of human diabetic patients: gene expression analysis of inflammatory biochemical markers. Lasers Med Sci. 33:165–171
17. Karu T (2013) Is it time to consider photobiomodulation as a drug equivalent? Photomed Laser Surg 31:189–191
18. Huang YY, Chen ACH, Carroll JD, Hamblin MR (2009) Biphasic dose response in low level lightherapy. Dose Response 7:358–383
19. Hamblin MR, Huang YY, Sharma SK, Carroll J (2011) Biphasic dose response in low level light therapy—an update. Dose Response 9:602–618
20. Naeser MA, Hamblin MR (2011) Potential for transcranial laser or LED therapy to treat stroke, traumatic brain injury, and neurodegenerative disease. Photomed Laser Surg 29:443–446
21. de Almeida TG, Alves MBR, Batissaco L, Torres MA, de Andrade AFC, Mingoti RD et al (2019) Does low-level laser therapy on degenerated ovine testes improve post-thawed sperm characteristics? Lasers Med Sci 34:1001–1009
22. Ravera S, Ferrando S, Agas D, De Angelis N, Raffetto M, Sabbieti MG et al (2019) 1064 nm Nd:YAG laser light affects transmembrane mitochondria respiratory chain complexes. J Biophotonics 12:1–7

23. Bossini PS, Muniz Renno AC, Ribeiro DA, Fangel R, Peitl O, Zanotto ED et al (2011) Biosilicate® and low-level laser therapy improve bone repair in osteoporotic rats. J Tissue Eng Regen Med 5:229–237
24. de Andrade ALM, Parisi JR, Parizotto NA, Luna GF, de Oliveira Leal ÂM, Brassolatti P et al (2018) Photobiomodulation effect on the proliferation of adipose tissue mesenchymal stem cells. Lasers Med Sci 34:677–683
25. Fávaro-Pípi E, Ribeiro DA, Ribeiro JU, Bossini P, Oliveira P, Parizotto NA et al (2011) Low-level laser therapy induces differential expression of osteogenic genes during bone repair in rats. Photomed Laser Surg 29:311–317
26. Tim CR, Bossini PS, Kido HW, Malavazi I, von Zeska Kress MR, Carazzolle MF et al (2016) Low-level laser therapy induces an upregulation of collagen gene expression during the initial process of bone healing: a microarray analysis. J Biomed Opt 21:088001–88009
27. Swatschek D, Schatton W, Kellermann J, Müller WEG, Kreuter J (2002) Marine sponge collagen: isolation, characterization and effects on the skin parameters surface-pH, moisture and sebum. Eur J Pharm Biopharm 53:107–113
28. Özel T, Bártolo PJ, Ceretti E, De Ciurana Gay JD, Rodríguez CA, Da Silva JVL (2016) Biomedical devices: design, prototyping, and manufacturing. Wiley, Hoboken, pp 1–190
29. Lopez-Heredia MA, Sa Y, Salmon P, De Wijn JR, Wolke JGC, Jansen JA (2012) Bulk properties and bioactivity assessment of porous polymethylmethacrylate cement loaded with calcium phosphates under simulated physiological conditions. Acta Biomater 8:3120–3127
30. Wang L, Yoon DM, Spicer PP, Henslee AM, Scott DW, Wong ME et al (2013) Characterization of porous polymethylmethacrylate space maintainers for craniofacial reconstruction. J Biomed Mater Res Part B Appl Biomater 101:813–825
31. Magri AMP, Fernandes KR, Kido HW, Fernandes GS, de Fermino S, Gabbai-Armelin PR, et al (2019) Bioglass/PLGA associated to photobiomodulation: effects on the healing process in an experimental model of calvarial bone defect. J Mater Sci Mater Med [Internet] 30:105–114. https://doi.org/10.1007/s10856-019-6307-x
32. Tim CR, Bossini PS, Kido HW, Malavazi I, von Zeska Kress MR, Carazzolle MF et al (2015) Effects of low-level laser therapy on the expression of osteogenic genes during the initial stages of bone healing in rats: a microarray analysis. Lasers Med Sci 30:2325–2333
33. Sarvestani FK, Dehno NS, Nazhvani SD, Bagheri MH, Abbasi S, Khademolhosseini Y et al (2017) Effect of low-level laser therapy on fracture healing in rabbits effect of low-level laser therapy on fracture healing in rabbits. Laser Ther 26:189–193
34. de Freitas NR, Guerrini LB, Esper LA, Sbrana MC, da Dalben G, Soares S et al (2018) Evaluation of photobiomodulation therapy associated with guided bone regeneration in critical size defects. In vivo study. J Appl Oral Sci 26:0244–255
35. de Oliveira LSS, de Araújo AA, de Araújo Júnior RF, Barboza CAG, Borges BCD, da Silva JSP (2017) Low-level laser therapy (780 nm) combined with collagen sponge scaffold promotes repair of rat cranial critical-size defects and increases TGF-β, FGF-2, OPG/RANK and osteocalcin expression. Int J Exp Pathol 98:75–85
36. Majidinia M, Sadeghpour A, Yousefi B (2018) The roles of signaling pathways in bone repair and regeneration. J Cell Physiol 233:2937–2948
37. Yang YQ, Tan YY, Wong R, Wenden A, Zhang LK, Rabie ABM (2012) The role of vascular endothelial growth factor in ossification. Int J Oral Sci 4:64–68
38. Zhou Y, Huang R, Fan W, Prasadam I, Crawford R, Xiao Y (2018) Mesenchymal stromal cells regulate the cell mobility and the immune response during osteogenesis through secretion of vascular endothelial growth factor A. J Tissue Eng Regen Med 12:e566–e578
39. Hosseinpour S, Fekrazad R, Arany PR, Ye Q (2019) Molecular impacts of photobiomodulation on bone regeneration: a systematic review. Prog Biophys Mol Biol 4:005–18